Journal of Applied Mechanics and Technical Physics, Vol. 46, No. 4, pp. 471–480, 2005

EVOLUTION OF A SMALL DISTORTION OF THE SPHERICAL SHAPE OF A GAS BUBBLE UNDER STRONG EXPANSION–COMPRESSION

A. A. Aganin and T. S. Guseva

UDC 534.2:532

The evolution of a small distortion of the spherical shape of a gas bubble which undergoes strong radial expansion–compression upon a single oscillation of the ambient liquid pressure under a harmonic law are analyzed by numerical experiments. It is assumed that the distortions of the spherical bubble shape are axisymmetric and have the form of individual spherical surface harmonics with numbers of 2–5. *Bubble-shape oscillations prior to the beginning of expansion are taken into account. Generally, the distortion value during bubble expansion–compression depends on the phase of bubble-shape oscillation at the beginning of the expansion* (*initial phase*). *Emphasis is placed on the dependence of the maximum distortions in the initial phase at certain characteristic times of bubble expansion–compression on the amplitude of the external excitation, liquid viscosity, and distortion mode* (*harmonic number*). *The parameters of the problem are typical of the stable periodic sonoluminescence of an individual air bubble in water at room temperature. An exception is the liquid pressure oscillation amplitude, which is varied up to values that are five times the static pressure. That large excitation amplitudes are beyond the stability threshold of periodic oscillations of spherical bubbles. Their consideration is of interest from the point of view of increasing the compression ratio of the bubble gas, i.e., increasing the maximum temperature and density achievable in the final compression stage.*

Key words: *bubble dynamics, distortion of the spherical shape, oscillations, sonoluminescence.*

Introduction. Numerous studies of the periodic sonoluminescence of an individual gas bubble in a liquid have shown [1] that at the moment of maximum compression, the state of the bubble gas is characterized by very high values of the density (10^3 kg/m^3) and temperature (10^4 K), which has led to increased interest in this phenomenon. Enhancing gas compression in the sonoluminescence mode has become one of the primary lines of research. In particular, Hingelfeldt et al. [2] proposed a simple model for the periodic sonoluminescence phenomenon and gave some recommendations on changing experimental conditions for the purpose of increasing the intensity of periodic bubble sonoluminescence. However, attempts to increase the maximum density and temperature of bubble gas in periodic oscillation modes have encountered various stability constraints [1, 2]. Therefore, studies aimed at increasing the compression ratio of bubble gas have begun in different modes of bubble oscillations, including the mode of periodically unstable, strong, single expansion–compression. Theoretical estimations using spherically symmetric models have shown [3] that in this mode of bubble dynamics, the maximum gas pressure and temperature are much higher than those achieved in the periodic sonoluminescence mode. The mode of single strong bubble expansion–compression was implied in the experimental facility whose design was proposed in [4]. However, for the first time it was implemented by Taleyarkhan et al. [5], who observed the release of neutrons and tritium nuclei under ultrasonic excitation (with an amplitude of 15 bar) of a bubble cluster in deuterated acetone.

Institute of Mechanics and Engineering, Kazan' Science Center, Russian Academy of Sciences, Kazan' 420111; aganin@kfti.knc.ru; guseva@kfti.knc.ru. Translated from Prikladnaya Mekhanika i Tekhnicheskaya Fizika, Vol. 46, No. 4, pp. 17–28, July–August, 2005. Original article submitted February 3, 2004; revision submitted August 10, 2004.

The results of [5] have sparked a lively discussion [6]. A number of critical comments concern the lack of estimates of the possibility of preserving the spherical bubble shape at the moment of its extreme compression. Indeed, a spherical or nearly spherical bubble shape is one of the most important conditions for achieving high compression ratios of bubble gas in any mode of radial bubble dynamics. The issue of the stability of the spherical shape has been studied the most thoroughly for expanding bubbles, compressing bubbles, and bubbles that undergo periodic expansion–compression. Emphasis has been given to determining the stability of the spherical bubble shape. A vast list of references is given in [7, 8]. Both analytical [9–12] and numerical methods of research have been employed. The stability of spherical oscillations of bubbles in the periodic sonoluminescence mode has been studied primarily numerically [8].

The present paper deals with studying the variation of small distortions of the spherical bubble shape in the case where all parameters of the problem correspond to the periodic sonoluminescence of an individual bubble and the liquid pressure oscillation amplitude is much (two or three times) higher. Under such excitation amplitudes, the periodic oscillations of a spherical bubble are unstable [13]. Therefore, we consider only a single bubble expansion–compression under a single simple harmonic oscillation of the liquid pressure which starts with a depression phase. It is assumed that prior to the beginning of expansion, the bubble surface performs undamped oscillations about the spherical state with a natural frequency that depends on the number of the spherical harmonic specifying the distortion mode, on the liquid density, surface tension, and the unchanged bubble radius. A similar situation arises, for example, at the end of each period of bubble oscillation at the center of a spherical flask in the periodic sonoluminescence mode, where radial oscillations of the bubble are already absent and its surface performs damped oscillations about the spherical state. In this case, liquid pressure variation near the bubble that ensures its strong expansion–compression can be implemented in the next oscillation period by an appropriate pressure pulse on the flask wall. A situation similar to the indicated one arises after damping of radial bubble oscillations produced by a laser breakdown in a liquid at the center of a spherical flask. In this case, the subsequent liquid pressure variation near the bubble can be caused by an incident spherical wave produced by an appropriate pressure pulse on the flask wall. In the formulation of the present work, the moment of the beginning of bubble expansion with respect to the phase of its shape distortion (initial phase) is considered arbitrary. Emphasis is placed on the variation of the distortions that are maximal in the initial phase. The damping of the bubble surface oscillations prior to the beginning of the expansion is ignored. As a result, the distortions that are maximal in the phase can be slightly overestimated.

In view of the small bubble size, considerable attention is paid to the effect of liquid viscosity. Fir this, the model of [14] and its simplified version ignoring the rotational motion of the liquid are used.

1. Mathematical Formulation of the Problem. A gas bubble is at the center of a spherical liquid volume. Prior to the beginning of pulsed action, the bubble radius does not change and its surface performs small undamped oscillations about the spherical state. At an arbitrary (with respect to the shape-oscillation phase) time, a long spherical wave is incident on the bubble, so that the ambient liquid pressure performs a single large-amplitude harmonic oscillation which starts with a depression. Because of the liquid pressure variation, the bubble is first strongly expanded and is then compressed even more strongly. This is followed by a number of rapidly damped radial oscillations of a relatively small amplitude. The variation of the maximum (in the initial phase) distortions of the spherical bubble shape is studied in the interval between the beginning of bubble expansion and the moment of its first extreme compression under the assumption that the distortions remain small.

The equation for the interface at an arbitrary time t in spherical coordinates r, θ, and φ is written as

$$r = R(t)\Big[1 + \sum_{i=2}^{\infty} \varepsilon_i(t) P_i(\cos\theta)\Big],$$

where R is the bubble radius, $P_i(\,\cdot\,)$ is a Legendre polynomial of order i, ε_i is the corresponding distortion of the spherical shape [inward, where $\varepsilon_i P_i(\cos\theta) < 0$, and outward, where $\varepsilon_i P_i(\cos\theta) > 0$]. Here and below, we use primarily nondimensional quantities. Dimensional quantities are denoted from below by an asterisk. In the nondimensionalizing procedure, the basic units are the liquid density ρ_{0*}, the initial bubble radius R_{0*}, and the characteristic velocity u_{0*}, which is defined by the expression $\sqrt{p_{0*}/\rho_{0*}}$, where p_{0*} is the static pressure of the liquid.

The distortions are assumed to be small ($|\varepsilon_i| \ll 1$). With this assumption and taking into account the liquid viscosity according to [14], the distortion ε_i is described by the equation

$$R\ddot{\varepsilon}_i + \Big[5\dot{R} + \frac{2(i+1)(i+2)}{\mathrm{Re}\,R}\Big]\dot{\varepsilon}_i + \Big[\frac{(i^2-1)(i+2)}{\mathrm{We}\,R^2} + \frac{3\dot{R}^2}{R} + \frac{6i(i+1)\dot{R}}{\mathrm{Re}\,R^2} - (i-2)\ddot{R}\Big]\varepsilon_i$$

$$+\frac{i(i+1)}{R}\Big[\frac{T_i(R,t)}{\mathrm{Re}\,R} + \frac{2(2i+1)R^{i-2}\alpha_i}{\mathrm{Re}} + \frac{\dot{R}}{R}\,\beta_i\Big] = 0, \tag{1}$$

$$\alpha_i = -\frac{i+1}{2i+1}\int\limits_R^\infty T_i(r,t)r^{-i}\,dr, \qquad \beta_i = \int\limits_R^\infty \Big[\Big(\frac{R}{r}\Big)^3 - 1\Big]\Big(\frac{R}{r}\Big)^i T_i(r,t)\,dr,$$

where $\mathrm{Re} = u_{0*}R_{0*}/\nu_*$, ν_* are the kinematic viscosity of the liquid, $\mathrm{We} = u_{0*}^2\rho_{0*}R_{0*}/\sigma_*$, and σ_* is the surface tension. The function $T_i(r,t)$ characterizes the rotational motion of the liquid. It is related to the liquid velocity $\boldsymbol{u}$ by the expression

$$\nabla\times\boldsymbol{u} = \nabla\times\Big(\sum_{i=2}^{\infty} T_i(r,t)P_i(\cos\theta)\Big)\boldsymbol{e}_1,$$

where $\boldsymbol{e}_1$ is the directing vector of the coordinate line r. The function $T_i(r,t)$ is determined from the equation

$$\frac{\partial T_i}{\partial t} + \dot{R}R^2\,\frac{\partial}{\partial r}\Big(\frac{T_i}{r^2}\Big) + \frac{1}{\mathrm{Re}}\Big(\frac{i(i+1)T_i}{r^2} - \frac{\partial^2 T_i}{\partial r^2}\Big) = 0 \tag{2}$$

subject to the boundary conditions

$$T_i(R,t) = 2\{(i+2)R\dot{\varepsilon}_i + 3\dot{R}\varepsilon_i + (2i+1)R^{i-1}\alpha_i\}/(i+1), \qquad T_i(\infty,t) = 0. \tag{3}$$

The integral expressions of α_i and β_i characterize the aggregate effect of the liquid vorticity on the bubble-shape oscillations. In this case, boundary condition (3) is implicit. As in a number of other studies (see, for example, [13]), an accounting of the liquid viscosity according to (1)–(3) will be called accurate.

The variation of the bubble radius R is described by the following equation for nondimensional quantities [15]:

$$\Big(1 - \frac{\dot{R}}{c_0} + \frac{4}{\mathrm{Re}\,c_0 R}\Big)R\ddot{R} + \frac{3}{2}\Big(1 - \frac{1}{3}\,\frac{\dot{R}}{c_0}\Big)\dot{R}^2 = \Big(1 + \frac{\dot{R}}{c_0}\Big)(p_\mathrm{b} - p_\infty) + \frac{R}{c_0}\,(\dot{p}_\mathrm{b} - \dot{p}_\infty) - \frac{4\dot{R}}{\mathrm{Re}\,R} - \frac{2}{\mathrm{We}\,R}, \tag{4}$$

where c_0 is the sound velocity in the liquid, p_b and p_∞ are the bubble gas pressure and the liquid pressure, respectively, at a large distance from the bubble, which are defined by the relations

$$p_\mathrm{b} = p_\mathrm{b}^0\Big(\frac{1-A}{R^3-A}\Big)^\gamma, \qquad p_\mathrm{b}^0 = 1 + \frac{2}{\mathrm{We}},$$
$$p_\infty = 1 - \Delta p\sin\omega t, \qquad 0 \leqslant t \leqslant 2\pi/\omega. \tag{5}$$

Here A is a constant and Δp and ω are the oscillation amplitude and frequency, respectively.

At $t < 0$, we set

$$\varepsilon_i(t) = \varepsilon_i^0\sin(\omega_i t + \varphi_0), \qquad \omega_i = \sqrt{(i^2-1)(i+2)/\,\mathrm{We}}\,,$$

and at $t = 0$,

$$R(0) = 1, \quad \dot{R}(0) = 0, \quad \varepsilon_i(0) = \varepsilon_i^0\sin\varphi_0, \quad \dot{\varepsilon}_i(0) = \dot{\varepsilon}_i^0\cos\varphi_0, \quad \dot{\varepsilon}_i^0 = \varepsilon_i^0\omega_i,$$
$$T_i(r,0) = T_{i,\varphi_0}(r), \tag{6}$$

where ε_i^0 and ω_i are the oscillation amplitude and frequency of the spherical bubble shape, respectively; $T_{i,\varphi_0}(r)$ is the radial distribution of the function T_i that corresponds to the initial phase φ_0. The initial phase φ_0 is arbitrary ($-\infty < \varphi_0 < \infty$).

Employing the finite-difference method to approximate the spatial derivatives in Eq. (2) and using quadrature formulas to approximate the integrals in the expressions for α_i and β_i, we reduce problem (1)–(6) to a system of ordinary differential equations for $\ddot{R}$, $\ddot{\varepsilon}_i$, and the grid values of the function $T_i(r,t)$. One of the difference equations for $T_i(r,t)$ follows from boundary conditions (3). The solution of the obtained system of equations is found numerically by the Dorman–Prince method [16].

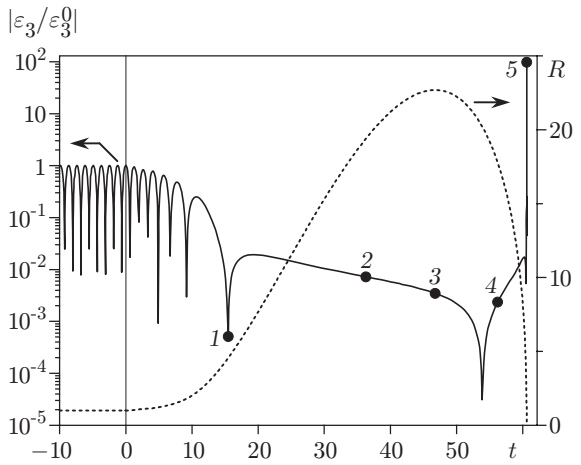

Fig. 1. Bubble radius R and the amplitude of relative distortion of the spherical bubble shape $|\varepsilon_3/\varepsilon_3^0|$ versus time for $\Delta p = 2$ ignoring the viscosity effect on the bubble shape (points 1–5 show a number of characteristic times).

The problem is considered for $p_{0*} = 10^5$ Pa, $\rho_{0*} = 1000$ kg/m^3, $R_{0*} = 4.5$ μm, $c_{0*} = 1500$ m/sec, $\omega_*/(2\pi) = 26.5$ kHz, $\nu_* = 10^{-6}$ m^2/sec, $\sigma_* = 0.073$ N/m, $A = 8.5^{-3}$, and $\gamma = 1.4$, which corresponds to the characteristic case of periodic sonoluminescence [1] where the air bubble is in water at room temperature. In the nondimensional variables, $c_0 = 150$, $\omega/(2\pi) \approx 1.2 \cdot 10^{-2}$, Re $= 45$, We ≈ 6, and $1.4 \leqslant \Delta p \leqslant 5$.

2. Effect of Bubble-Shape Oscillations prior to the Beginning of Expansion. Figure 1 gives the most typical time dependences of the bubble radius and the relative distortion of its spherical shape before and during strong single expansion–compression for the problem parameters considered. Points 1–5 denote the times t_{1-5}, among which t_1, t_2, and t_4 are characteristic for the solutions of Eq. (1) and t_3 and t_5 correspond to the maximum expansion and maximum compression of the bubble. At the beginning of the expansion stage, the distortion of the spherical bubble shape varies in a damped oscillation mode with an increasing period. At the time t_1, the variation of the distortion enters a damping mode without oscillations (the aperiodic damping mode) and is considerably slowed down. In the interval t_2–t_3, the distortion again varies in a damped oscillation mode but with a very large period. The stage of bubble compression starts with a slow variation of the distortion in a growing oscillation mode. The rate of variation in the distortion increases rapidly as the compression rate becomes higher. At the time t_4, the distortion variation enters a mode of increase without oscillations (the aperiodic growth mode). In this regime, the distortion amplitude varies at increasing rate and with several very sharp changes in the direction of increase in the distortion: growth of the distortion into the interior of the bubble is replaced by its increase outward and vice versa. In the stage of accelerated compression, an increase in the distortion of the spherical bubble shape is due to Birkhoff–Plesset type instability [10, 11]. An especially rapid increase in the distortion occurs at the final, very short, segment of the decelerating bubble compression. This is related to the development of Rayleigh–Taylor instability [11, 17]. The indicated features in the bubble shape variation are characteristic of all examined harmonic numbers i on most of the range $1.4 \leqslant \Delta p \leqslant 5$. We note that at the very end of the compression stage, the employed model of bubble dynamics may be not quite adequate. In particular, here the liquid compressibility effect near the bubble, which is ignored in the present work, can become significant. Therefore, the results pertaining to the moment of the maximum compression (collapse) of the bubble should be treated as an estimate.

Figure 2 gives curves of the relative distortion $\varepsilon_2/\varepsilon_2^0$ at the moment of bubble collapse versus the pressure variation amplitude Δp ignoring the effect of liquid viscosity on the bubble shape variation. It is evident that there is a strong dependence of the distortion value on φ_0. Thus, for $\Delta p \approx 3$, the distortion at the moment of collapse for $\varphi_0 = \pi/2$ is close to zero, and for $\varphi_0 = 0$, it exceeds the initial value by a factor of approximately 80. A strong dependence of the distortion value on φ_0 is also observed at other times of the expansion–compression. It is also preserved in the case of accounting for the liquid viscosity.

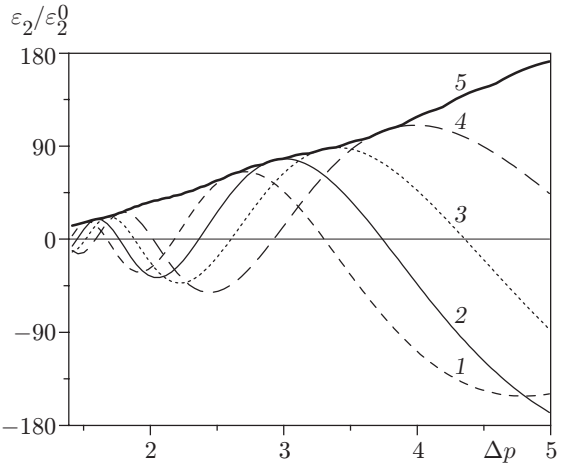

Fig. 2. Relative distortion of the spherical bubble shape $\varepsilon_2/\varepsilon_2^0$ for $\varphi_0 = -\pi/4$, 0, $\pi/4$, and $\pi/2$ (curves 1–4, respectively) and the relative distortion of the spherical shape $\varepsilon_{2mc}/\varepsilon_2^0$ with the maximum φ_0 (curve 5) versus Δp at the time of bubble collapse ignoring the viscosity effect on the bubble shape.

Below, we consider the variation of the distortion $\varepsilon_{im}(t)$ that at the time t is maximal among the values of $\varepsilon_i(t)$ that correspond to $-\infty < \varphi_0 < \infty$. For brevity, the parameter $\varepsilon_{im}(t)$ is called the maximum distortion. We use the designations $\varepsilon_{imm} = \varepsilon_{im}(t_m)$ and $\varepsilon_{imc} = \varepsilon_{im}(t_c)$, where t_m and t_c are the times of the maximum bubble expansion and maximum compression, respectively. With allowance for periodicity in φ_0, the set $-\infty < \varphi_0 < \infty$ is replaced by a discrete set of points Φ_0 on the half-period $-\pi/2 \leqslant \varphi_0 \leqslant \pi/2$. In Fig. 2, curve 5 shows the relative maximum distortion at the time $t = t_c$. It is evident that it differs markedly from curves 1–4, in particular, in that its values are positive everywhere and increase monotonically.

3. Dependence of Maximum Distortions on Radial Motion. The effect of the radial bubble dynamics on the bubble shape variation during expansion–compression is estimated using a formulation ignoring the effect of liquid viscosity on the distortion. In this case, relation (1) reduces to the equation

$$R\ddot{\varepsilon}_i + 5\dot{R}\dot{\varepsilon}_i + \Big[\frac{(i^2-1)(i+2)}{\mathrm{We}\,R^2} + \frac{3\dot{R}^2}{R} - (i-2)\ddot{R}\Big]\varepsilon_i = 0. \tag{7}$$

Using (7) for $i = 2$, we find that the aperiodic damping mode during bubble expansion arises for all Δp in the range $1.4 \leqslant \Delta p \leqslant 5$, and for $i = 3$, 4, and 5 it is absent for $\Delta p < 1.5$, 1.8, and 2.1, respectively.

Figure 3a gives curves of the ratio $\varepsilon_i^0/\varepsilon_{imm}$, which characterizes the damping ratio of the maximum distortions in the expansion stage (ε_i^0 is the maximum initial distortion) versus the amplitude Δp for various values of i. For $\Delta p = 1.4$, the values of $\varepsilon_i^0/\varepsilon_{imm}$ are close for all i. As Δp increases to 1.9, 2.3, and 3.1, the increase in the damping ratio is more considerable for harmonics $i = 3$, 4, and 5, respectively, than for $i = 2$; for $i \geqslant 3$ in the indicated intervals, it changes almost equally. In the case of further increase in Δp, where a rather long aperiodic mode is already observed for $i \geqslant 3$ in the expansion stage, the damping ratio for $i = 2$ continues to increase, and for $i \geqslant 3$, it remains constant ($i = 3$) or decreases monotonically ($i = 4$ and 5). Thus, as the harmonic number i increases, the nature of the dependence of the damping ratio $\varepsilon_i^0/\varepsilon_{imm}$ on the excitation amplitude Δp varies. For $i = 2$, it is monotonically increasing; as i increases, the monotonicity is gradually violated. For $i = 5$ and $\Delta p \approx 3$, a distinct maximum is already observed. The least damping of the maximum distortions in the interval $1.4 \leqslant \Delta p \leqslant 5$ is observed for $i = 2$: by a factor of approximately 60 for small Δp and by a factor of almost 110 for large Δp. With increase in the harmonic number i, the damping ratio of the maximum distortions in the expansion stage increases on most of the examined range of Δp. In particular, for $\Delta p = 5$, it increases from ≈110 ($i = 2$) to ≈230, 500, and 1400 ($i = 3$, 4, and 5, respectively).

For $i = 2$, the rate of variation of the maximum distortion at the time t_m (i.e., at the beginning of the compression stage) decreases monotonically in the range $1.4 \leqslant \Delta p \leqslant 5$ (Fig. 3b). For $i = 4$ and 5, it also decreases for small Δp for which the aperiodic damping mode is absent. Next, in the intervals $1.8 < \Delta p < 2.3$ for $i = 4$ and $2.2 < \Delta p < 3.3$ for $i = 5$, where a short aperiodic mode already occurs in the expansion stage, the value of $|\dot{\varepsilon}_{im}/\varepsilon_i^0|$

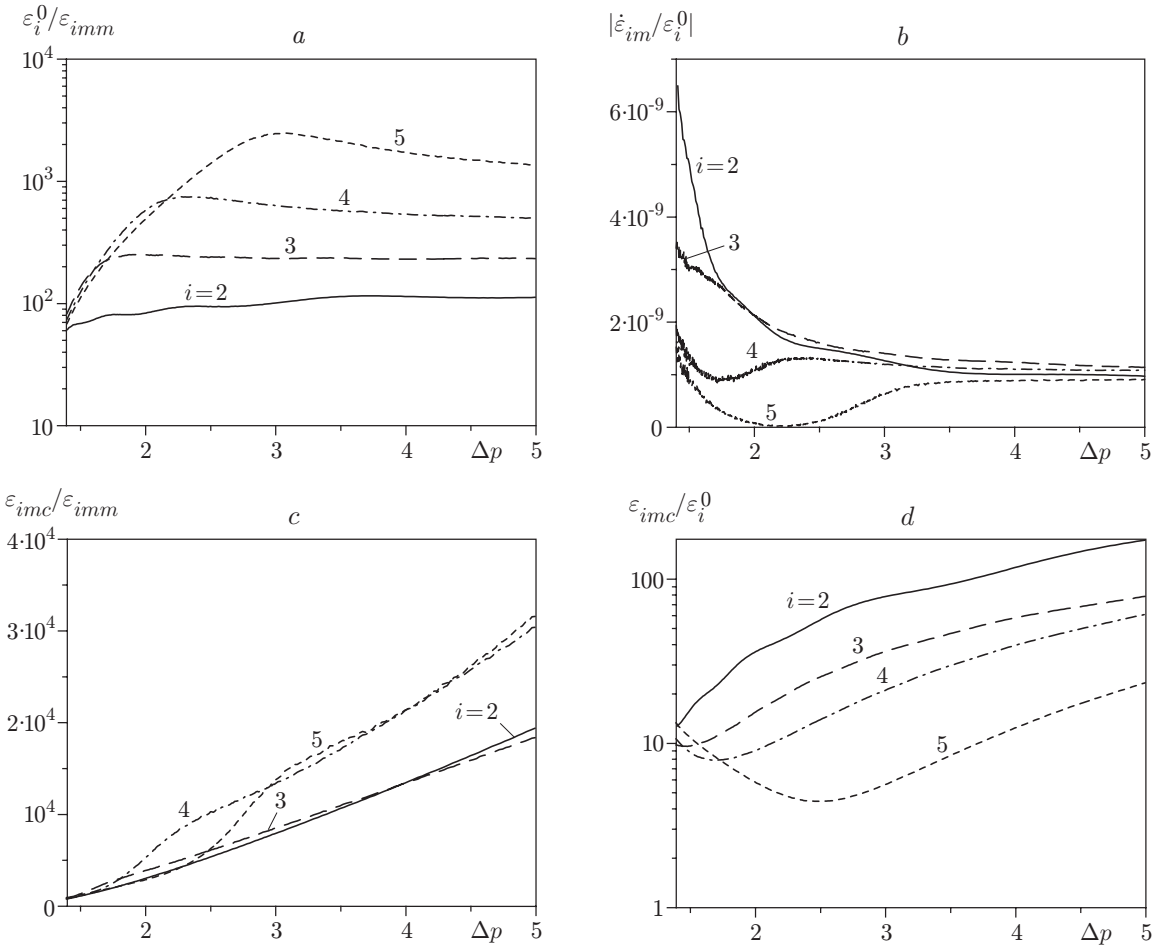

Fig. 3. Damping ratio of the maximum distortions in the stage of bubble expansion $\varepsilon_i^0/\varepsilon_{imm}$ (a), the modulus of the relative rate of change in the maximum distortion at the end of the expansion stage $|\dot\varepsilon_{im}/\varepsilon_i^0|$ (b), and the growth ratio of the maximum distortions in the compression stage $\varepsilon_{imc}/\varepsilon_{imm}$ (c) and during the entire expansion–compression process $\varepsilon_{imc}/\varepsilon_i^0$ (d) versus Δp for harmonics $i = 2$–5.

increases notably. With further increase in Δp for $i = 4$ and 5, the rate of variation of the maximum distortions at the end of the expansion stage decreases ($i = 4$), like for $i = 2$, 3, or increases slightly ($i = 5$). On the final segment $4 \leqslant \Delta p \leqslant 5$, its values are close for all i.

Figure 3c gives curves of the ratio $\varepsilon_{imc}/\varepsilon_{imm}$ versus Δp for various values of i. This ratio characterizes the growth ratio of the maximum distortions in the compression stage. As is evident from Fig. 3a and b, over the entire range $1.4 \leqslant \Delta p \leqslant 5$ and for all i, the ratio $\varepsilon_{imc}/\varepsilon_{imm}$ exceeds $\varepsilon_i^0/\varepsilon_{imm}$, i.e., the growth of the maximum distortions for compression exceeds their damping for expansion. In the range of small Δp, the values of $\varepsilon_{imc}/\varepsilon_{imm}$ for $i = 2$–5 are close, in particular, for $\Delta p = 1.4$, we have $\varepsilon_{imc}/\varepsilon_{imm} \approx 800$. With increase in Δp, the growth ratio of the maximum distortions under compression $\varepsilon_{imc}/\varepsilon_{imm}$ for $i = 2$ and 3 increases to approximately $2 \cdot 10^4$ for $\Delta p = 5$ under a nearly linear law. For $i = 4$ and 5, the ratio $\varepsilon_{imc}/\varepsilon_{imm}$ increases much faster in the intervals of Δp in which there is an increase in the variation rate of the maximum distortions at the beginning of the compression stage $|\dot\varepsilon_{im}/\varepsilon_i^0|$ (see Fig. 3b). At the end of these intervals, the increase in the growth ratio of the maximum distortions under compression $\varepsilon_{imc}/\varepsilon_{imm}$ slows down, and up to the end of the examined range of variation of Δp, it occurs similarly to that for $i = 2$ and 3. In this case, the values of $\varepsilon_{imc}/\varepsilon_{imm}$ for $i = 4$ and 5 are close and exceed the values of this ratio for $i = 2$ and 3 by a factor of approximately 1.6–1.7.

Figure 3d shows curves of the ratio $\varepsilon_{imc}/\varepsilon_i^0$ versus Δp for $i = 2$–5. This ratio characterizes the growth ratio of the maximum distortions during the entire bubble expansion–compression process from the initial moment of

expansion $t = 0$ to the moment of the maximum compression (collapse) $t = t_c$. The value of $\varepsilon_{imc}/\varepsilon_i^0$ is determined by the ratio of the damping ratio of the maximum distortions for expansion to the growth intensity for compression. The largest values of $\varepsilon_{imc}/\varepsilon_i^0$ correspond to the harmonic with a number $i = 2$, for which the least damping of the maximum distortions in the expansion stage is observed. The value of $\varepsilon_{2mc}/\varepsilon_2^0$ increases monotonically from approximately 12.3 at the beginning of the range of variation of Δp to almost 170 at the end. With increase in i, the monotonicity in the growth of $\varepsilon_{imc}/\varepsilon_i^0$ is increasingly violated. In the region of small Δp, the increase in the damping ratio of distortions under expansion with increase in Δp exceeds the increase in the growth rate under compression (for $i = 3$, they nearly compensate for each other); therefore, in this region, the growth rate of the maximum distortions by the moment of collapse $\varepsilon_{imc}/\varepsilon_i^0$ for $i = 4$ and 5 decreases. In the neighborhood of values $\Delta p \approx 1.8$ for $i = 4$ and $\Delta p \approx 2.4$ for $i = 5$, the increase in the growth ratio of the maximum distortions for compression $\varepsilon_{imc}/\varepsilon_{imm}$ is notably accelerated (see Fig. 3c), and this is responsible for the presence of distinct minima in the curve of $\varepsilon_{imc}/\varepsilon_i^0$ versus Δp, after which the growth ratio of the maximum distortions under expansion–compression $\varepsilon_{imc}/\varepsilon_i^0$ increases monotonically. Subsequently, its growth is partly determined by a decrease in the damping ratio of the maximum distortions under expansion (Fig. 3a).

For $\Delta p > 1.8$, the growth ratio of the maximum distortions during bubble expansion–compression decreases with increase in the harmonic number i. In particular, for $\Delta p = 5$, it decreases from ≈170 for $i = 2$ to ≈80, 61, 23 for $i = 3$, 4, 5 respectively.

4. Dependence of the Maximum Distortions on Liquid Viscosity. To analyze the effect of liquid viscosity on the distortion of the spherical bubble shape, we use the solutions of the problem obtained with an accurate accounting of this factor [Eqs. (1)–(3)], ignoring it [Eq. (7)], and ignoring the rotational motion of the liquid, in which case system (1)–(3) reduces to the equation

$$R\ddot{\varepsilon}_i + \Big[5\dot{R} + \frac{2(i+1)(i+2)}{\operatorname{Re} R}\Big]\dot{\varepsilon}_i + \Big[\frac{(i^2-1)(i+2)}{\operatorname{Re} R^2} + \frac{3\dot{R}^2}{R} + \frac{6i(i+1)\dot{R}}{\operatorname{Re} R^2} - (i-2)\ddot{R}\Big]\varepsilon_i = 0. \tag{8}$$

An approximate allowance for the effect of liquid viscosity (8) only leads to a small change in the values of Δp indicated above for Eq. (7) for which there is the aperiodic damping mode for $i = 3$, 4, and 5 in the stage of bubble expansion.

Figure 4 gives the results of calculations using Eqs. (1)–(3) (solid curves) and Eq. (8) (dashed curves). The wavy nature of the curves is due to the disagreement between the oscillation frequency of the bubble shape at $t < 0$ and the damped oscillation frequency at the beginning of the expansion stage; with an accurate allowance for the viscosity in the cases $i = 4$ and 5 for small Δp, it is also due to the rotational motion of the liquid. The latter turns out to be significant at the end of the damped oscillation mode in the expansion stage. In this case, the rotational motion prevents the growth of distortions of the spherical bubble shape with deviations from this shape in the same direction (into the interior of the bubble or outward) as for the initial distortion, and the damping of distortions that are opposing in this respect.

A comparison of the results presented in Fig. 3a and 4a suggests that the effect of liquid viscosity leads to a strong increase in the damping ratio of the maximum distortions in the bubble-expansion stage $\varepsilon_i^0/\varepsilon_{imm}$ for all harmonic numbers i. The minimum increase in the damping ratio occurs for $i = 2$ and decreases considerably as Δp increases. Thus, the damping ratio $\varepsilon_2^0/\varepsilon_{2mm}$ obtained with an accurate allowance for the viscosity effect is larger than that ignoring viscosity by a factor of almost 24 for $\Delta p = 1.4$ and by a factor of approximately 2.2 for $\Delta p = 5$. The contribution of the rotational motion of the liquid is small and also decreases with increase in Δp. Neglect of the rotational motion results in a change in the damping ratio $\varepsilon_2^0/\varepsilon_{2mm}$ from ≈30% for small Δp to ≈15% for large.

As the harmonic number i increases, the effect of liquid viscosity for bubble expansion becomes even more significant, especially in the range of small Δp. The effect of the rotational motion of the liquid also increases. Thus, in the case $i = 5$, the damping ratio $\varepsilon_i^0/\varepsilon_{imm}$ with an accurate allowance for viscosity is larger than that ignoring viscosity by a factor of $\approx 7 \cdot 10^4$ time for $\Delta p = 1.4$ and by a factor of ≈50 for $\Delta p = 5$; in addition, it also larger than that in the case of ignoring the rotational motion by a factor of ≈3.5 for $\Delta p = 1.4$ and by a factor of ≈1.5 for $\Delta p = 5$. The most considerable peaks of the curves of $\varepsilon_i^0/\varepsilon_{imm}$ for $i = 4$ and 5 at the beginning of the range of Δp are due to the effect of the rotational motion of the liquid.

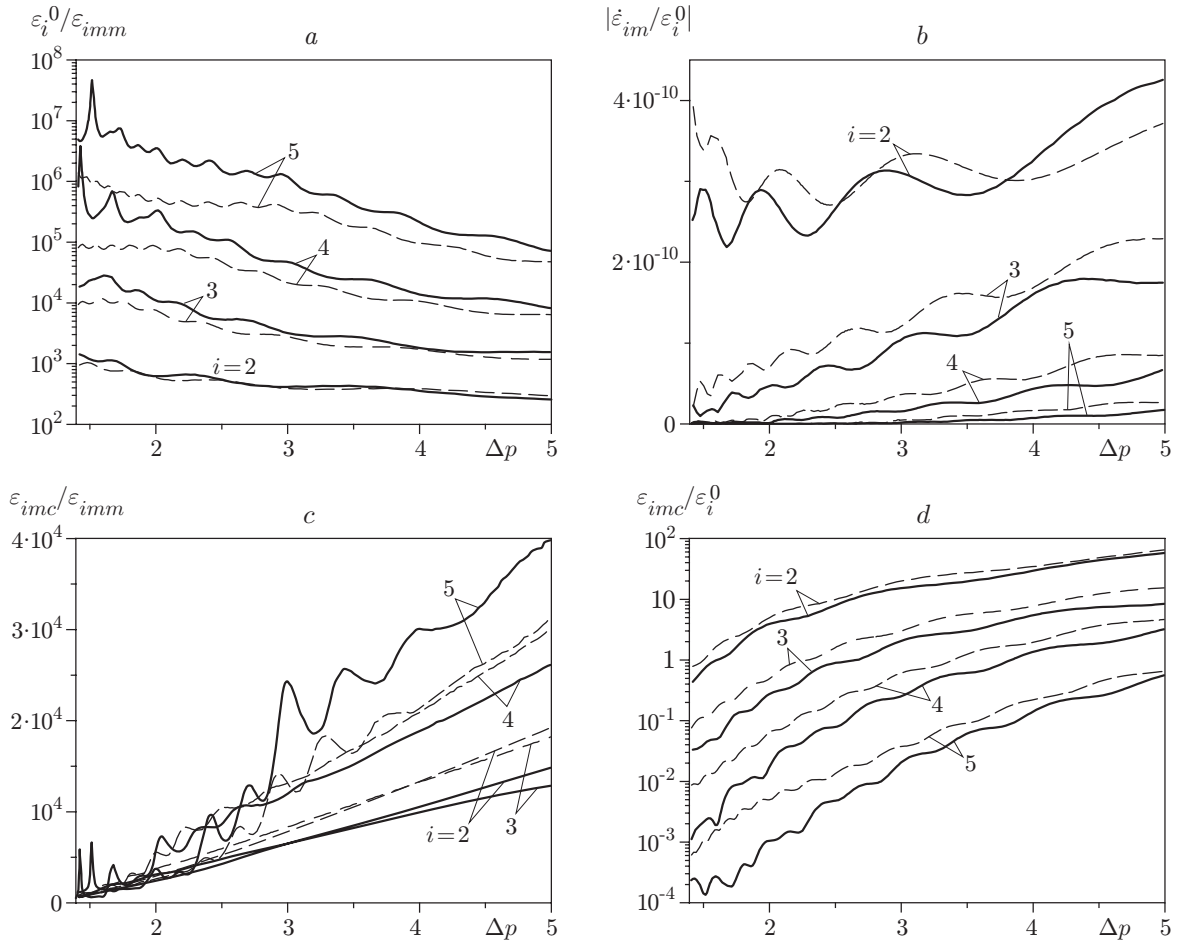

Fig. 4. Same as in Fig. 3 but with an accurate allowance for the effect of liquid viscosity on the bubble shape (solid curves) and an approximate description ignoring the rotational motion of the liquid (dashed curves).

As is evident from Fig. 4b, both the accurate and approximate methods of allowing for the liquid viscosity lead to a considerable decrease in the rate of variation of the maximum distortions at the moment of the maximum bubble expansion $|\dot\varepsilon_{im}/\varepsilon_i^0|$. At the same time, unlike in the case of an inviscid liquid, the average rate $|\dot\varepsilon_{im}/\varepsilon_i^0|$ for $i = 2$ and 3 increases with increase in Δp (except for the harmonic $i = 2$ ignoring the rotational motion in the region of small Δp). For $i = 4$ and 5 in the region of small Δp where there is no aperiodic damping mode, the average value of $|\dot\varepsilon_{im}/\varepsilon_i^0|$ remains nearly constant, and its increase begins for those values of Δp for which the aperiodic mode of distortion damping occurs in the expansion stage.

From a comparison of Figs. 3c and 4c, it can be concluded that in the bubble compression stage, the effect of liquid viscosity is less significant than that during bubble expansion. In this case, unlike in the expansion stage, it is due mainly to the rotational motion of the liquid. Thus, for $i = 2$ with accurate allowance for viscosity, the growth of the maximum distortions under compression $\varepsilon_{imc}/\varepsilon_{imm}$ is $\approx 6 \cdot 10^2$ for $\Delta p = 1.4$ and $\approx 1.5 \cdot 10^4$ for $\Delta p = 5$, which is approximately 1.3 times smaller than that ignoring viscosity. At the same time, the dependences of $\varepsilon_{2mc}/\varepsilon_{2mm}$ on Δp obtained ignoring the rotational motion [Eq. (8)] and with complete neglect of viscosity [Eq. (7)] differ insignificantly. An almost the same situation is observed for $i = 3$ in the interval $1.4 \leqslant \Delta p \leqslant 5$ and for $i = 4$, 5 in the region of large Δp.

It is interesting that for $i = 2{-}4$, the effect of the rotational motion of the liquid leads to a reduction in the growth ratio of the maximum distortions $\varepsilon_{imc}/\varepsilon_{imm}$ on most of the examined range of Δp, whereas in the case $i = 5$, this effect leads to its increase, which is specially considerable for large Δp. Thus, for $\Delta p = 5$, the value

of $\varepsilon_{5mc}/\varepsilon_{5mm}$ obtained with an accurate allowance for viscosity is ≈20% larger than that obtained ignoring the rotational motion of the liquid.

In addition, it is remarkable that in the accurate method [Eqs. (1)–(3)] and approximate method [Eq. (8)] of allowing for liquid viscosity for small Δp and in the middle of the interval $1.4 \leqslant \Delta p \leqslant 5$, the nature of variation in $\varepsilon_{imc}/\varepsilon_{imm}$ is more nonmonotonic for harmonics $i = 4$ and 5 than for $i = 2$ and 3. In the case of allowing for liquid viscosity, the occurrence of peaks in the region of small Δp is due to the presence of peaks in the corresponding curves of $\varepsilon_i^0/\varepsilon_{imm}$ (see Fig. 4a). In the middle of the interval Δp, namely, where the ratio $\varepsilon_{imc}/\varepsilon_{imm}$ increases more rapidly, like in the case of ignoring viscosity, the indicated nonmonotonicity is due to the nonmonotonic dependence of the oscillation phase of the maximum distortion at the time t_m on Δp.

With an accurate allowance for liquid viscosity, the growth ratio of the maximum distortions during expansion–compression $\varepsilon_{imc}/\varepsilon_i^0$ over the entire examined range of Δp for all $i = 2{-}5$ is slightly smaller than that ignoring the rotational motion of the liquid and is much smaller than that with complete neglect of viscosity (see Fig. 3d and 4d). Ignoring the wavy nature of the corresponding curves in Fig 4d, it can be concluded that the indicated differences decrease with increase in Δp and increase with increase in i. In particular, for $\Delta p = 1.4$ and $i = 5$, neglect of only the rotational motion of the liquid leads to an overestimation of the value of $\varepsilon_{imc}/\varepsilon_i^0$ by a factor of approximately 2.5, and complete neglect of viscosity leads to an overestimation by a factor of almost $5.5 \cdot 10^4$. For $\Delta p = 5$ and $i = 2$, this overestimation decreases by a factor of almost 1.1 and 3, respectively.

Thus, according to Fig. 4d, in the examined interval $1.4 \leqslant \Delta p \leqslant 5$ with an accurate allowance for viscosity, an increase in the maximum distortions during bubble expansion–compression occurs only for $i = 2$, 3, and 4 with $\Delta p > 1.6$, 2.7, and 3.9, respectively. In the case $i = 5$, the maximum distortion at the moment of collapse is everywhere smaller than the initial value. The largest value of the growth ratio of the maximum distortions during bubble expansion–compression $\varepsilon_{imc}/\varepsilon_i^0 \approx 60$ is reached for $i = 2$ and $\Delta p = 5$.

Conclusions. The nature and degree of variation of a small distortion of the spherical shape of a gas bubble subjected to a strong single expansion–compression in a liquid are studied in the case where all problem parameters correspond to the periodic sonoluminescence of an individual bubble and the liquid pressure oscillation amplitude is two or three times as large. At such excitation amplitudes, the periodic oscillations of the spherical bubble are unstable. The study was performed with allowance for the bubble-shape oscillations prior to the beginning of expansion. The shape variation of the bubble surface was analyzed on the basis of distortions that are maximal in the initial phase.

It was established that the distortion of the spherical bubble shape first strongly decreases in the expansion stage and then strongly increases in the compression stage. For all examined harmonic numbers $i = 2{-}5$, the damping ratio of the maximum distortion in the expansion stage decreases with increase in the liquid pressure oscillation amplitude Δp; in contrast, the growth ratio of the maximum distortion under compression increases. As the harmonic number i increases, the damping ratio of the maximum distortion under expansion increases considerably. Ultimately, during bubble expansion–compression from the initial time of expansion to the moment of the maximum compression (collapse), the growth ratio of the distortion of the spherical bubble shape increases as the liquid pressure oscillation amplitude Δp increases and as the harmonic number i decreases in their examined ranges.

The effect of liquid viscosity was studied. In the bubble expansion stage, it considerably raises the damping ratio of the maximum distortion. In this case, the contribution of the rotational motion due to liquid viscosity is small, especially for small i. In the bubble compression stage, the viscosity effect is much less significant and is determined primarily by the rotational motion of the liquid. Depending on the harmonic number, it can favor both a reduction and an increase in the growth ratio of the maximum distortion. The liquid viscosity effect becomes less pronounced as Δp increases and as i decreases.

This work was supported by the Russian Foundation for Basic Research (Grant No. 02-01-00100) within the framework of the program of the Branch of Physical and Technical Problems of Energetics of the Russian Academy of Sciences, and the Integration Federal target program (Grant No. B0020).

REFERENCES

1. B. P. Barber, R. A. Hiller, R. Lofstedt, et al., "Defining the unknowns of sonoluminescence," *Phys. Rep.*, **281**, 65–143 (1997).
2. S. Hilgenfeldt, S. Grossman, and D. Lohse, "Sonoluminescence light emission," *Phys. Liquids*, **11 (6)**, 1318–1330 (1999).
3. A. A. Aganin and M. A. Ilgamov, "Dependence of bubble compression parameters on the external pressure," in: *Dynamics of Multiphase Systems*, Proc. Int. Conf. on Multiphase Systems, Ufa (2000), pp. 269–274.
4. V. A. Simonenko, V. N. Nogin, Y. A. Kucherenko, et al., "Single bubble collapse: Physics and prospects," *ibid*, pp. 306–315.
5. R. P. Taleyarkhan, C. D. West, J. S. Cho, et al., "Evidence for nuclear emissions during acoustic cavitation," *Science*, **295**, 1868–1873 (2002).
6. C. Seife, "'Bubble fusion' paper generates a tempest in a beaker," *ibid*, pp. 1808–1809.
7. A. A. Aganin and M. A. Il'gamov, "Gas bubble dynamics in a viscous liquid with considerable distortions of the spherical shape," in: *Dynamics of Gas Bubbles and Aerosols* [in Russian], Izd. Kazan. Gos. Univ., Kazan', (2003), pp. 7–22.
8. S. J. Putterman and K. R. Weninger, Sonoluminescence: How bubbles turn sound into light," *Annu. Rev. Liquid Mech.*, **32**, 445–476 (2000).
9. V. K. Andreev, *Stability of Unsteady Free-Boundary Fluid Flows* [in Russian], Nauka, Novosibirsk (1992).
10. M. S. Plesset and T. P. Mitchell, "On the stability of the spherical shape of a vapor cavity in a liquid," *Quart. J. Appl. Math.*, **13 (4)**, 419–430 (1956).
11. O. V. Voinov and V. V. Perepelkin, "Stability of the surface of a gas bubble pulsating in a liquid," *J. Appl. Mech. Tech. Phys.*, No. 3, 410–416 (1989).
12. O. V. Voinov, "Breakdown of bubbles: Non-linear mechanisms and effects," in: *Proc. of the Third Int. Conf. on Multiphase Flow*, ICMF'98, Lyon, France, June 8–12 (1998).
13. C. C. Wu and P. H. Roberts, "Bubble shape instability and sonoluminescence," *Phys. Lett. A*, **250**, 131–136 (1998).
14. A. Prosperetti, "Viscous effects on perturbed spherical flows," *Quart. Appl. Math.*, **34**, 339–352 (1977).
15. J. B. Keller and M. Miksis, "Bubble oscillations of large amplitude," *J. Acous. Soc. Am.*, **68 (2)**, 628–633 (1980).
16. E. Hairier, S. P. Norsett, and G. Wanner, *Solving Ordinary Differential Equations: Nonstiff Problems*, Springer-Verlag (1987).
17. G. Taylor, "The instability of liquid surfaces when accelerated is perpendicular to their planes," *Proc. Roy. Soc.*, **A201**, 192 (1950).